The Mansurov Effect: Real or a statistical artefact?

Jone Edvartsen[1], Ville Maliniemi[2], Hilde Nesse Tyssøy[3], Timo Asikainen[4], and Spencer Mark Hatch[5]

[1]Birkeland Center for Space Science
[2]University of Bergen
[3]Birkeland Centre for Space Science, Dept. of Physics and Technology, University of Bergen
[4]Space Physics and Astronomy Research Unit, University of Oulu
[5]Birkeland Centre for Space Science

November 24, 2022

Abstract

The Mansurov Effect is related to the interplanetary magnetic field (IMF) and its ability to modulate the global electric circuit, which is further hypothesized to impact the polar troposphere through cloud generation processes. In this paper we investigate the connection between IMF By-component and polar surface pressure by using daily ERA5 reanalysis for geopotential height since 1980. Previous studies have shown to produce a significant 27-day cyclic response during solar cycle 23. However, when appropriate statistical tests are applied, the correlation is not significant at the 95\% level. Our results also show that data from three other solar cycles, which have not been investigated before, produce similar cyclic responses as during solar cycle 23, but with seemingly random offset in the timing of the signal. We examine the origin of the cyclic pattern occurring in the super epoch/lead lag regression methods commonly used to support the Mansurov hypothesis in all recent papers, as well as other phenomena in this community. By generating random normally distributed noise with different levels of temporal autocorrelation, and using the real IMF By-index as forcing, we show that the methods applied to support the Mansurov hypothesis up to now, are highly susceptible, as cyclic patterns always occurs as artefacts of the methods. This, in addition to the lack of significance, suggests that there is no adequate evidence in support of the Mansurov Effect.

The Mansurov Effect: Real or a statistical artefact?

Edvartsen, J.[1], Maliniemi, V.[1], Nesse Tyssøy, H.[1], Asikainen, T.[2] and Hatch, S.[1]

[1]Birkeland Center for Space Science, Department of physics and technology, University of Bergen
[2]Space Physics and Astronomy Research Unit, University of Oulu, Oulu, Finland

Key Points:

- We review the Mansurov Effect of interplanetary magnetic influence on Antarctic surface pressure
- Different sub-periods over the last 40 years give an inconsistent surface pressure response
- IMF B_y influence is seen only during solar cycle 23, but careful examination shows it is not statistically significant

Abstract

The Mansurov Effect is related to the interplanetary magnetic field (IMF) and its ability to modulate the global electric circuit, which is further hypothesized to impact the polar troposphere through cloud generation processes. In this paper we investigate the connection between IMF B_y-component and polar surface pressure by using daily ERA5 reanalysis for geopotential height since 1980. Previous studies have shown to produce a significant 27-day cyclic response during solar cycle 23. However, when appropriate statistical tests are applied, the correlation is not significant at the 95% level. Our results also show that data from three other solar cycles, which have not been investigated before, produce similar cyclic responses as during solar cycle 23, but with seemingly random offset in the timing of the signal. We examine the origin of the cyclic pattern occurring in the super epoch/lead lag regression methods commonly used to support the Mansurov hypothesis in all recent papers, as well as other phenomena in this community. By generating random normally distributed noise with different levels of temporal autocorrelation, and using the real IMF B_y-index as forcing, we show that the methods applied to support the Mansurov hypothesis up to now, are highly susceptible, as cyclic patterns always occurs as artefacts of the methods. This, in addition to the lack of significance, suggests that there is no adequate evidence in support of the Mansurov Effect.

1 Introduction

First proposed in 1974, the Mansurov Effect is based on the correlation between daily polar surface pressure and the B_y-component of the interplanetary magnetic field (IMF). Significant correlation has been shown in multiple studies (Mansurov et al. 1974; Burns et al. 2008; Lam et al. 2013; Lam et al. 2014). Evidence of significant ionospheric perturbations related to the same change in B_y also exists (Tinsley 2000; 2008; Frank-Kamenetsky et al. 2001; Kabin et al. 2003; Pettigrew et al. 2010; Lam et al. 2013). A physical mechanism involving the Global Electric Circuit (GEC) modulating cloud generation processes has been suggested to link IMF B_y to the polar surface pressure (Lam and Tinsley 2016). However, research on the linkage between the GEC and cloud generation is severely limited. Laken et al. (2012) found no apparent significant relationship between solar/and or cosmic rays and the modulation of cloud generation through the GEC.

The theory predicts a positive (negative) relation between the IMF B_y-component and the polar surface pressure/geopotential height in the southern hemisphere (northern hemisphere) (Burns et al. 2008). The impact on the cloud formation and the pressure should occur with a lag of less than a day, first detectable in the lower troposphere (Lam et al. 2014). Mansurov et al. (1974) found correlations between IMF B_y and surface pressure in the time period around 1956 to 1964 (approximately solar cycle 19). Later publications focus on the period 1999–2002 (Burns et al. 2008; Lam et al. 2013; Lam et al. 2014). This time interval produces high statistical significance in both hemispheres. Burns et al. (2008) (hereafter B2008) also extends the time interval to 1995–2005, where statistical significance is found in the southern hemisphere (SH), but not in the northern hemisphere (NH). To our knowledge, analyses of the effect in other time periods have not been published.

Two different methods are typically applied to derive this effect. The first is the superposed epoch method (Mansurov et al. 1974; Lam et al. 2013; Lam et al. 2014). The pressure/geopotential height on days with strong B_y deflections (usually $|B_y| > 3$ nT) are binned according to the sign of B_y. The difference between the two bins are shown as lead-lags relative to the forcing on a daily scale. The second method is lead-lag regression plots (B2008). Here, the average pressure/geopotential height is calculated in five B_y bins, and the slope of the regression line between the average B_y and the average pressure/geopotential height in each bin is calculated and plotted for chosen daily leads and lags. We emphasise that both methods yield approximately the same results, as the slope of the regression line strongly depends on the pressure/geopotential height in the lowest and highest B_y bins.

In this paper we revisit the Mansurov hypothesis and previous applied methods with a more rigorous estimate of the statistical significance. Emphasis is also put on time periods other than solar cycle 23 (1995–2005). In addition, we examine the lead-lag regression method with the help of Monte Carlo simulations and randomly generated normally distributed temporally uncorrelated (white) noise and autocorrelated (red) noise. The aim is to demonstrate the need for appropriate significance tests, as well as the risk of misinterpreting a response from strongly periodic forcing, when assessing the impact of Space on Earth.

2 Data

2.1 Solar wind (B_y) data

We use hourly averaged IMF B_y values obtained from the National Space Science Data Center (NSSDC) OMNIWeb database (https://omniweb.gsfc.nasa.gov) for the interval 1980–2016. IMF B_y daily averages are calculated when at least 20 hourly values are available.

2.2 Pressure/Geopotential height data

For the atmospheric data, we use the European Center for Medium-Range Weather Forecast Re-Analysis (ERA5) (https://cds.climate.copernicus.eu). We obtain the daily averaged geopotential heights at the 700 hPa (SH) and 1000 hPa (NH) level poleward of 70° in geomagnetic coordinates (mlat), covering the time period 1980-2016. Geomagnetic coordinates are used as the perturbation of IMF B_y in the ionosphere is centered around the geomagnetic pole. For comparison, B2008 used surface pressure measurements obtained for 11 Antarctic sites from the NNDC (NOAA [National Oceanic and Atmospheric Administration] National Data Centers), selecting values within 90 min of 12 UT. Also, as an analogue to the quantity Δp that B2008 calculate, a variation value ΔZ_g is obtained for the geopotential height by subtracting a running mean of $\pm$15 days in order to remove seasonal variability. It is noted that ΔZ_g is averaged over 70-90 degrees mlat.

Figure 1 shows the temporal autocorrelation in ΔZ_g for the period 1980–2016 in the SH. Positive self-correlation occurs until day 5. A similar autocorrelation is also found for the period 1995–2005, as well as for ΔZ_g in the NH.

3 Analyses and Results

3.1 Regression results for the time period 1995–2005

Based on observations from the 11 Antarctic stations, B2008 calculated the average Δp values at each site within five separate IMF By bins: < -3, -3 to -1, -1 to 1, 1 to 3, and >3 nT. Linear regression was then applied to the average value of Δp within these five intervals. The result for >83°S mlat, corresponding to the upper panel of Figure 1 in B2008, is shown in the left panel in Figure 2. The same procedure is done for ΔZ_g, seen in the middle panel in Figure 2. Also included is a linear regression without the initial binning and averaging, seen in the right panel in Figure 2. Note that the regression coefficients are similar with or without performing the initial binning, while the explanatory value of the model R^2 differs substantially.

From the regression coefficient produced by these five data bins, lead-lag variations are calculated by B2008, as seen in the left panel of Figure 3. A clear 27-day cycle is seen for both data sets, with the peak pressure value lagging the driver by -2 days. The significance has been estimated by Student's t-test. Figure 2 and 3 indicate that ΔZ_g yields a similar response as Δp in B2008. Furthermore, note that the normal regression without the initial grouping gives similar lead-lag regression coefficients.

When applying the t-test, a highly significant pattern is observed, as shown in Figure 3. However, the lead-lag analysis is strongly affected by the temporal autocorrelation in the ΔZ_g time series (Figure 1). Instead of a t-test we therefore perform a Monte Carlo (MC) simulation to estimate the significance of the regression coefficients. For every iteration of the MC-simulation, phase randomization is applied to the ΔZ_g data series. In essence, phase randomization scrambles the harmonic phases of the series. This results in a physically unrelated data series, but preserves the autocorrelation function of ΔZ_g, which gives the phase randomized series the same number of independent data points as ΔZ_g. This process ensures that the MC simulation can perform the null hypothesis test on statistically suitable material (Theiler et al. 1996; Thejll et al. 2003). The B_y series is then regressed onto the phase randomized ΔZ_g for every lead-lag. The original regression coefficient is then compared to the distribution of coefficients obtained from the MC simulation in each lead-lag to obtain a fraction of more extreme values. This represents the p-value.

Figure 4 shows the results after 3000 iterations of the MC simulation. The green shaded area shows the interval corresponding to 95% of the values from all iterations. The red shaded area shows above(below) the 97.5%(2.5%) percentile, corresponding to a p-value smaller or equal 0.05 (two-tailed t-test). As can be seen, the significance is reduced compared to what is obtained by the t-test. Also, the peak around day 0 is only

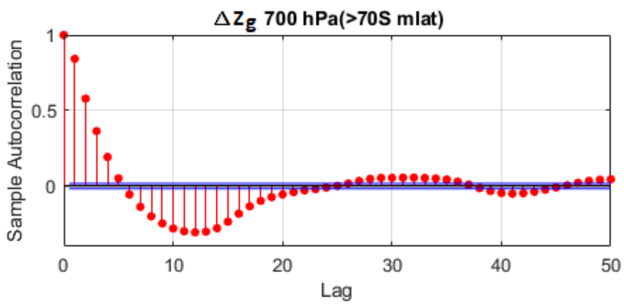

Figure 1. Temporal autocorrelation of ΔZ_g over the period 1980–2016. Positive self-correlation occurs until day 5.

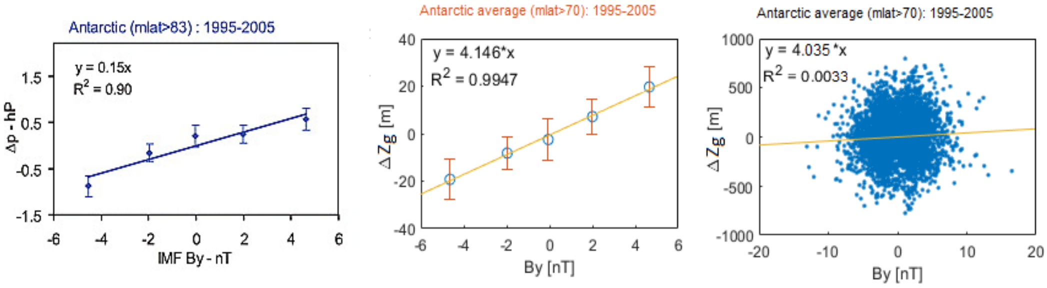

Figure 2. **Left panel**: A copy of the upper panel of Figure 1 in B2008. It represents linear regression of Δp after the original measurement from three Antartic stations at mlat >83°S was grouped according to the IMF By. **Middle panel**: Reproduction of the linear regression method using ΔZ_g at ∼mlat >70°S. Error bars are plus/minus one standard-error-in-the-mean. **Right panel**: Scatter plot and linear regression for the ΔZ_g data without the initial five-bin grouping. The upper panel of Figure 1 in B2008 is reproduced with permission from John Wiley and Sons.

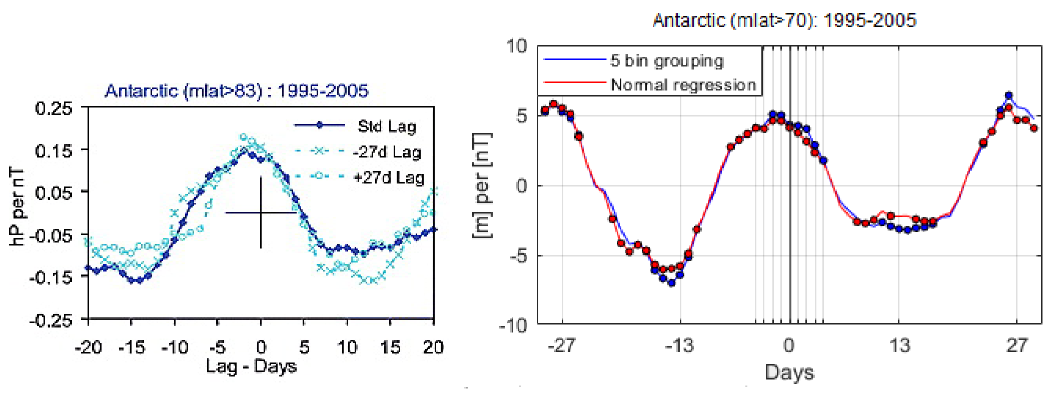

Figure 3. **Left panel**: A copy of the upper panel of Figure 2 in B2008. The figure illustrates calculated regression coefficients showing lead-lag variations of Δp at mlat >83°S. It shows three cycles of IMF B_y, where the dark blue line represents the regression coefficients without any lag, while x and o cyan lines represents a -27 and +27 day lag between IMF B_y and Δp data series. All maxima in Δp are seen to occur -2 days before the peak in the IMF driver, which occurs at day 0. **Right panel**: Lead-lag variations of ΔZ_g at mlat >70°S. The blue line is the calculated regression coefficients showing lead-lags when the five bin method by B2008 is used. The red line is the regression coefficients showing lead-lag variations when regression is done without the initial grouping. Negative days (leads) represent ΔZ_g occurring before the B_y component, and positive days B_y occurring before ΔZ_g. Dots indicate significance at the 95% level for the regression coefficients calculated by Student's t-test. The upper panel of Figure 2 in B2008 is reproduced with permission from John Wiley and Sons.

found significant at the 95% level for two data points, occurring at day -2 and -1. However, multiple points with 95% significance are obtained at the peaks around -27 and +27 days, along with the minimum around -13 days. Note that the y axis in Figure 4 shows the correlation coefficient, i.e., how many standard deviations ΔZ_g increase per one standard deviation increase in B_y. For day -2 the correlation coefficient is equal to 0.064: for days -15, -27, and +27, it is approximately 0.08. This implies that B_y can explain less than one percent of the pressure variability (R^2 <0.01).

B2008 cite the apparent periodic response in Figure 4 as support for B_y forcing. Rigorous statistical testing of this apparent periodic response requires assessment of all individual hypothesis tests (for each lead/lag point) as a whole, i.e., estimating the global significance limit. Interpretation of individual hypothesis test by rejecting the null hypothesis with a p-value of 0.05 is that there is 5% probability of erroneously rejecting the null hypothesis. Thus, with multiple individual hypothesis tests the probability of erroneously rejecting an individual hypothesis test increases with the number of individual tests (Wilks 2016). To overcome this issue, Wilks (2016) provides a method known as False Detection Rate (FDR). It is stated that if the global null hypothesis cannot be rejected, one cannot conclude that any of the individual tests constitute rejection of the null hypothesis. In this case, the global null hypothesis is that there is no significant response formed from the lead-lag regression coefficients. Thus, according to FDR, the p-value is first calculated for each individual data point. The p-values are then sorted in ascending order, matching the set i = 1,..,N, where N represents the total number of individual tests. The new global p-value, $\mathrm{p}_{\mathrm{FDR}}$;

$$\mathrm{p}_{\mathrm{FDR}} = \max[\mathrm{p}(i) : \mathrm{p}(i) \leq (i/\mathrm{N})\alpha_{\mathrm{FDR}}],\ i = 1, .., \mathrm{N} \tag{1}$$

is then calculated with $\alpha_{\mathrm{FDR}} = 0.05$, corresponding to significance at the 95% level (Wilks 2016).

When the FDR method is applied, no significance is obtained at the 95% level for any lead-lag in the period 1995–2005. This occurs because no p-value of any lead-lag is able to fulfill the requirements for the rejection of the global null hypothesis, stated in Equation 1. This is true whether we calculate $\mathrm{p}_{\mathrm{FDR}}$ for lead-lags -27 to +27, -13 to +13 or even for -2 to +2. This means that the response as a whole cannot be assumed to be statistically significant. One must note though that if only a single lead or lag (e.g., leads -2 or -1) is presented the significance at the 95% level is justified (see Equation 1). However, from a physical perspective it is hard to justify the response occurring 1 or 2 days (or more than 12 days) before the forcing instead of at day 0 or after.

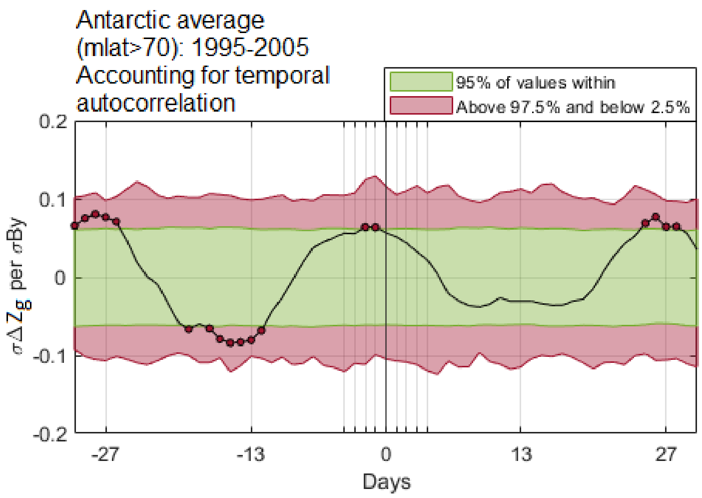

Figure 4. The significance level for the lead-lag regression coefficients after 3000 MC-iterations for the period 1995–2005. The red area equates to a p-value of 0.05. The green region shows where 95% of all values land for every lead-lag after 3000 iterations. The y-axis represents the correlation coefficient. Note that the significant data points (red circles) represent individual hypothesis tests before False Detection Rate method is applied.

Figure 5 shows the same procedure for the period 1999–2002 previously investigated by e.g. Burns et al. (2008), Lam et al. (2013) and Lam et al. (2014). After 3000 MC iterations, only 1 significant data point remains close to day 0 in the SH (top left panel) and in the NH (top right panel). However, application of FDR shows that no leads or lags that by themselves are above the 95% significance level constitute evidence in favor of rejecting the global null hypothesis in any of the hemispheres (bottom panels). This is true whether we calculate p_{FDR} for lead-lags -27 to +27, -13 to +13 or even for -2 to +2 (+2 to +6 for the SH). Although, the correlation coefficients for this period is in line with a physical effect, as the peak ΔZ_g anomaly occurs after day 0 in both hemispheres, it is not significant in regards to rejection of the global null hypothesis.

3.2 Other time periods

Figure 6 shows the standardized lead-lag regression coefficients (correlation) between ΔZ_g and $\mathrm{B_y}$ for the periods 1984–1994, 1995–2005 and 2006–2016 in both hemispheres (top panels). The bottom panels show the same, only for 4-year periods centered around four different solar maxima. Near all of the time periods in both hemispheres show cyclic responses exhibiting a periodicity of ∼27 days. However, none of the time periods outside of solar cycle 23 (1995–2005 or 1999–2002) show responses supported by the theory (positive response in the SH and negative response in the NH at day zero or shortly after). Instead, the peaks occur seemingly at random but with an apparent periodicity of approximately 27 days.

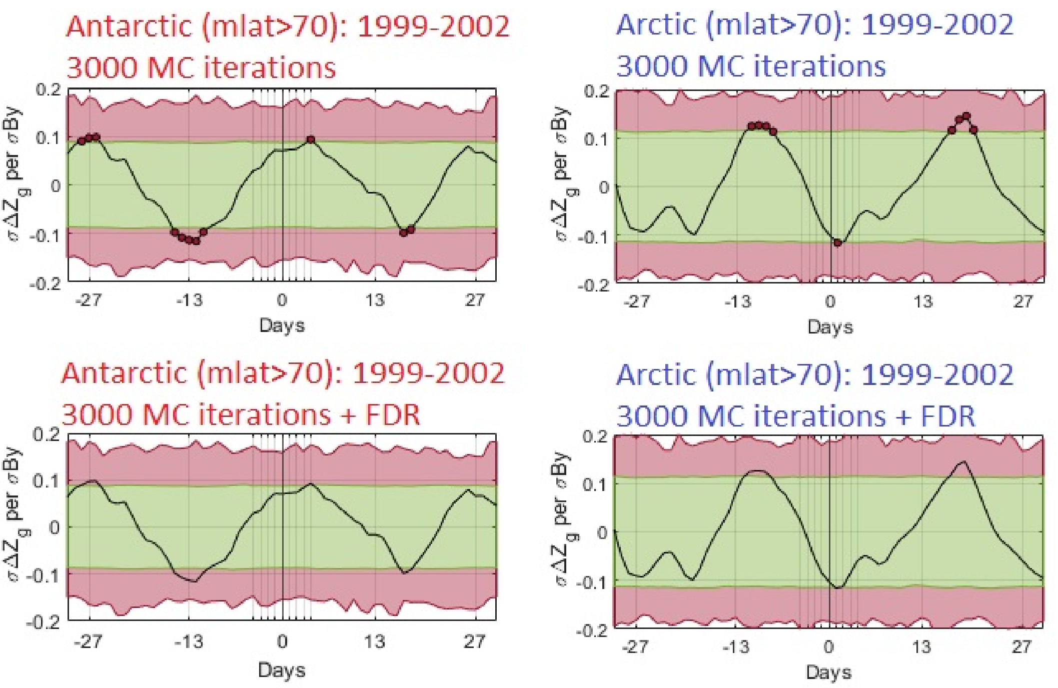

Figure 5. Left Panels: The significance level for the lead-lag regression coefficients after 3000 MC-iterations for the period 1999–2002 in the SH. Red circles indicate 95% significance of the individual hypothesis tests (top panel). No significance is obtained after FDR. This is the case whether FDR is computed for -27 to +27, -13 to +13 or +2 to +6 (bottom panel). **Right Panels:** Same procedure, only for the NH (top panel). No significance is obtained after FDR. This is the case whether FDR is computed for -27 to +27, -13 to +13 or -2 to +2 (bottom panel).

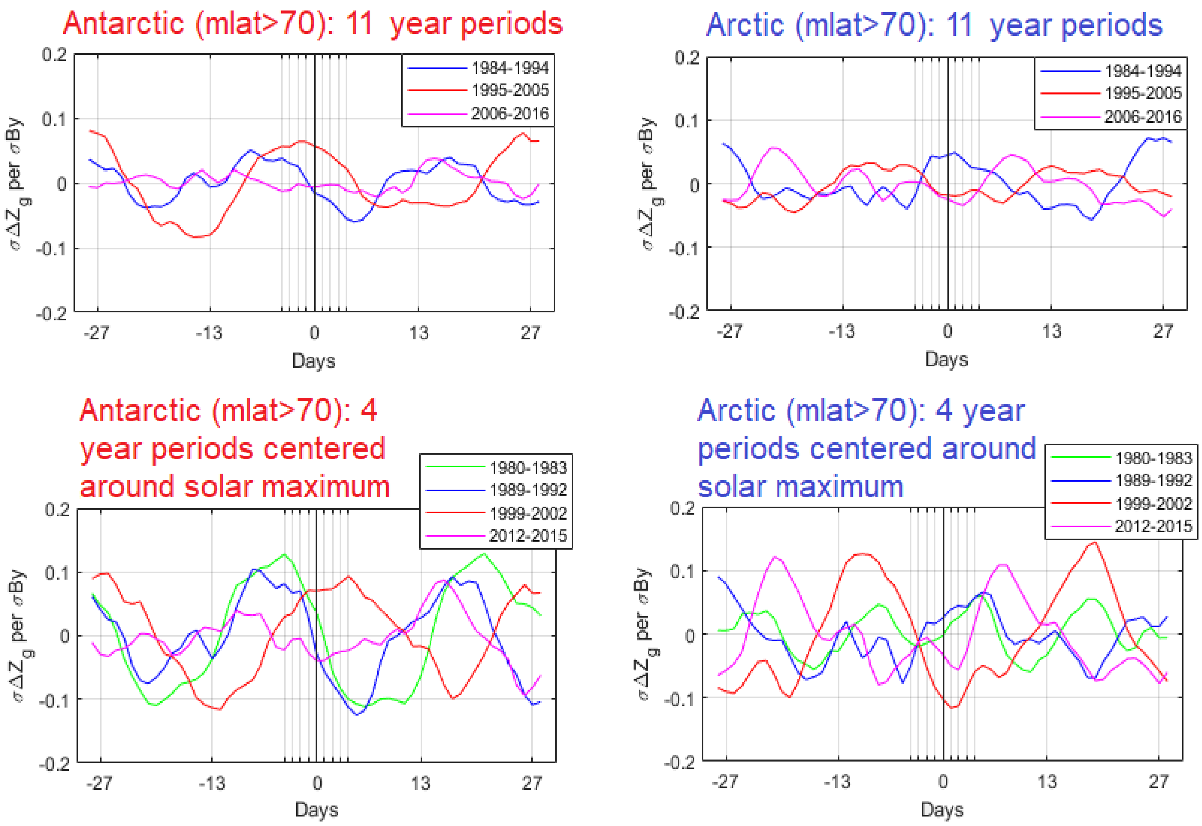

Figure 6. Lead-lag correlation coefficients between ΔZ_g and B_y in both hemispheres for three 11-year periods spanning 1984–2016 (top panels), and four 4-year periods centered around solar maximum (bottom panels).

3.3 Monte Carlo simulations with different levels of temporal autocorrelation

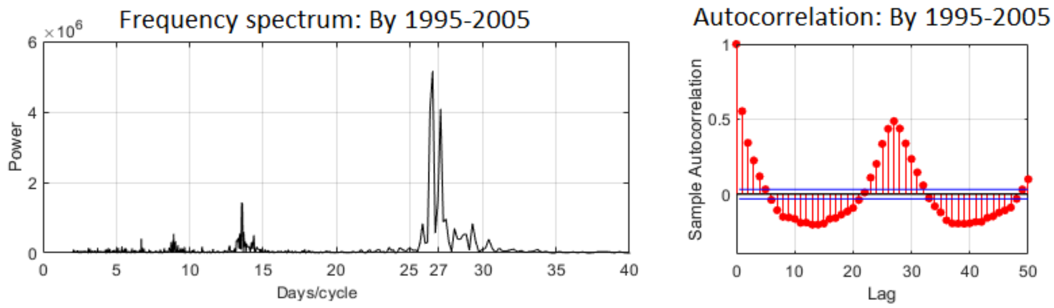

Figure 7. **Left Panel:** Frequency analysis of the IMF By-index in the time period 1995–2005. **Right Panel:** Autocorrelation function of the IMF By-index in the time period 1995–2005.

Figure 6 demonstrates that the periodic response in ΔZ_g of ~27 days is not unique to the 1995–2005 period, as it occurs in other time periods as well. Since the responses do not seem to have any relation to the forcing (day 0), could the resulting cyclic response be an artifact of the method itself, combined with high temporal autocorrelation of the explanatory variable?

Figure 7 shows the frequency spectrum (left panel) together with the autocorrelation function (right panel) of the IMF B_y over the time period 1995–2005. A strong 27-day solar rotation periodicity can be observed in both. When the regression coefficients for lead-lag variations are calculated, one data set is moved with respect to the other, where the regression coefficient is calculated for each lag between the data sets. In essence, this can lead to the responses seen at day $\pm$ 27 days, being partially replications of the response seen at day 0, occurring as a consequence of the periodicity of the forcing. This is especially relevant if the response variable has a strong temporal autocorrelation.

To demonstrate this, we calculate three Monte Carlo simulations with varying levels of autocorrelation of the response variable. For all cases the geopotential height data set is replaced by randomly generated normally distributed noise with the same length as the 1995–2005 period. For the first, second and third case, lag-1 autocorrelation is set to 0, 0.5 and 0.94, respectively. An autocorrelation of 0 represents a data set of normally distributed white noise, while the autocorrelation of 0.94 reflects the autocorrelation seen in the original geopotential height data series (not shown). The $\pm$ 15 day moving average is further subtracted from the three random data series, analogue to the calculation of ΔZ_g.

For all three cases, 1000 independent Monte Carlo iterations are run. For each run we calculate the lead-lag regression coefficients between the real B_y forcing in the period 1995-2005, and the random generated data series. Figure 8 summarizes the results. The first column represents the lead-lag regression coefficients for all runs in the three cases. It is noted that the same scaling is used for the y-axis, to yield the correlation coefficient R. The lead-lag curves appear to be random. However, if each curve is shifted such that the maximum value occurring inside the range (-13,13) days from day 0 is shifted to day 0, a pattern emerges. This is illustrated in the middle row of panels. When the responses are averaged over all independent simulations, as shown at right, the resulting average lead-lag curve exhibits a periodicity equal to the periodicity of B_y. It is furthermore apparent that the higher the autocorrelation of the random data series at lag-1, the larger the amplitudes of the artificially created response. It is particularly interesting that the correlation coefficients in Figure 6 are comparable to the correlation coefficients resulting from the third artificial case (lag-1 autocorrelation = 0.94) in Figure 8.

Figure 8 clearly shows that the 27-day cyclic response in surface pressure to the B_y-component cannot be used as a strong argument supporting the Mansurov Effect. Furthermore, it clearly demonstrates the necessity of using FDR or a similar method when estimating the significance of the response.

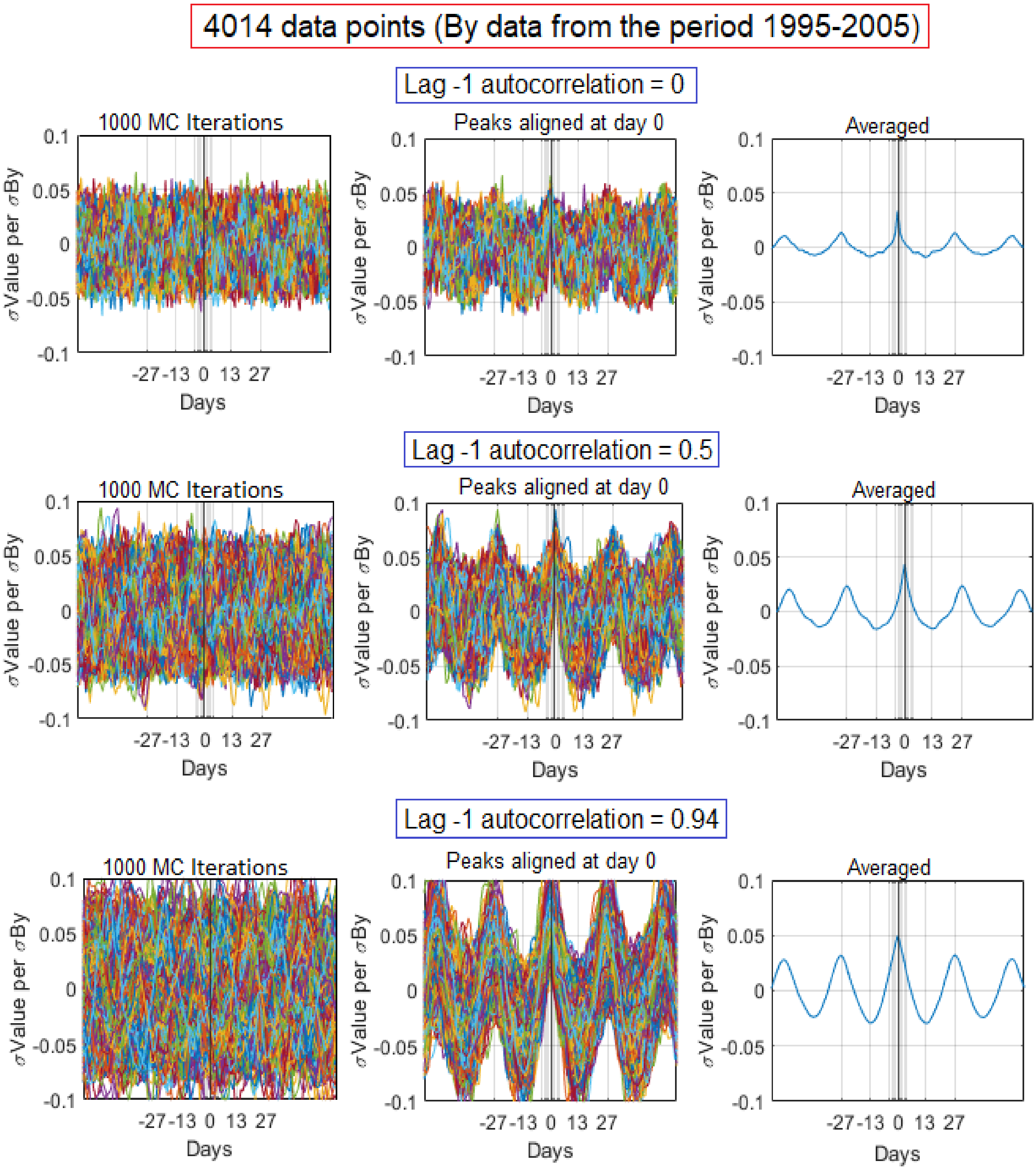

Figure 8. Left Panels: 1000 MC iterations where the standardized regression coefficients are calculated between the real B_y data for the period 1995–2005 and the three different random cases for every lead lag between -60 to +60. **Middle Panels**: All 1000 individual lead-lag plots aligned such that the maximum value within -13 to +13 is projected to day 0. **Right Panels:** Averaged response of the middle panels.

4 Discussion

The aim of this paper is to demonstrate the need for appropriate significance tests, as well as the risk of misinterpreting a response from a strongly periodic forcing when studying the Mansurov Effect (and also more generally in cases of strong temporal autocorrelation). Figure 2 shows that similar values for the regression slopes are obtained with five-bin grouping used by B2008 and the normal regression. However, the explanatory power of the two models largely depends on whether or not the measurements are binned (with binning $R^2 = 0.99$, without binning $R^2 = 0.0033$). Further, both the five-bin grouping and the normal regression produce similar lead-lag plots, as illustrated by Figure 3. It is therefore clear that the five-bin grouping gives the impression of a significantly better fit than what can be found in the original data.

Except for the first paper on the effect, provided by Mansurov et al. (1974), all other research articles focuses on solar cycle 23 (B2008; Lam et al. 2013; Lam et al. 2014). We show, however, that simple t-tests are not sufficient to establish significance for the link between the IMF B_y and the geopotential height variability at the polar surface. By applying MC simulations to validate the null hypotheses in addition to false detection rate method, we show that neither the period 1995-2005 nor the solar maximum period 1999–2002 indicate a statistically significant response. This remains true as long as the response is analysed with multiple leads and lags exceeding or equalling 5 days, as the individual p-values exceeds the global p-value (Equation 1) even for -2 to +2 lead-lags in all cases for solar cycle 23. Nonetheless, if only a single lead or lag is presented, the significance at the 95% level obtained by the MC simulation alone would be justified. During the period 1995–2005 the points with high statistical significance at leads -2 or -1 are hard to justify on physical grounds, as the surface pressure effect occurs before the forcing. However, the single significant data point obtained in the SH (day +4) and NH (day +1) for the period 1999-2002 cannot be completely discarded from the viewpoint of a single null hypothesis, as the effect occurs after the forcing.

By similar methodology, we also observe periodic geopotential height responses in both hemispheres in other time periods, but with varying offset in respect to the forcing, as illustrated by Figure 6. The geopotential height deflections are also fairly equal to the amplitudes seen for solar cycle 23. Hence, the cyclic responses seen in solar cycle 23 are not unique to this period.

By using MC simulations of randomly generated data series with different levels of lag-1 autocorrelation, we show that plotting lead-lag regression coefficients for a highly periodic forcing produces periodic responses, even when no physical relationship is present (Figure 8). The periodic response always mimic the periodicity of the variable used as the forcing. One can also observe how this cyclic response is enhanced by a higher autocorrelation of the response variable. From this perspective, the alignment of the period 1999–2002 with the theory is a coincidence (1995-2005 is also approximately aligned with the theory in the SH). The absence of any rejection of the global null hypothesis of the response in solar cycle 23 when FDR is applied is clear additional evidence in favor of this explanation.

4.1 Conclusion

We question the previous evidence suggesting a physical link between the IMF B_y and the surface pressure/geopotential height variability. We show that after the pressure/geopotential height and IMF B_y data are subjected to rigorous estimation of statistical significance, evidence for the Mansurov Effect during solar cycle 23 is not found. This applies for the cyclic 27-day response. In addition, our analyses shows that other time periods (before and after solar cycle 23) produce cyclic responses with similar magnitude but with random offset with respect to the IMF B_y forcing. We also provide evidence showing that high temporal autocorrelation of variables can explain the cyclic responses, without the need of a physical connection between the variables. We therefore question the validity of the Mansurov hypothesis.

5 References

[1] Burns, G.B., Tinsley, B.A., French, W.J.R., Troshichev, O.A. Frank-Kamenetsky, A.V. (2008), Atmospheric circuit influences on ground-level pressure in the Antarctic and Arctic, *J. Geophys. Res.*, 113, D15112

[2] Frank-Kamenetsky, A.V., Troshichev, O.A., Burns, G.B. Papitashvili, V.O. (2001), Variations of the atmospheric electric field in the near-pole region related to the interplanetary magnetic field, *J. Geophys. Res.*, 106, 179-190

[3] Kabin, K., Rankin, R., Marchand, R., Gombosi, T.I., Clauer, C.R., Ridley, A.J., Papitashvili, V.O. DeZeeuwk, D.L. (2003), Dynamic response of Earth's magnetosphere to By reversals, *J. Geophys. Res.*, 108, 1-13

[4] Laken, B.A., Pallé, E., Calogovic, J. Dunne, E.M. (2012), A cosmic ray-climate link and cloud observations, *J. Space Weather Space Clim.* 2. A18

[5] Lam, M.M., Chisham, G. Freeman, M. (2013). The interplanetary magnetic field influences mid-latitude surface atmospheric pressure. *Environmental Research Letters.* 8.

[6] Lam, M.M., Chisham, G. Freeman, M.P. (2014), Solar-wind-driven geopotential height anomalies originate in the Antarctic lower troposphere. *Geophys. Res. Lett.* 41

[7] Lam, M.M. Tinsley, B.A. (2016). Solar wind-atmospheric electricity cloud microphysics connections to weather and climate. *Journal of Atmospheric and Solar-Terrestrial Physics*, ISSN: 1364-6826, Vol: 149, 277-290

[8] Lam, M.M., Freeman, M. Chisham, G. (2018). IMF-driven change to the Antarctic tropospheric temperature due to the global atmospheric electric circuit. *Journal of Atmospheric and Solar-Terrestrial Physics.* 180, 148-152

[9] Mansurov, S.M., Mansurova, L.G., Mansurov, G.S., Mikhnevich, V.V. Visotsky, A.M. (1974), North-south asymmetry of geomagnetic and tropospheric events. *Journal of Atmospheric and Terrestrial Physics.* 36(11), 1957-1962

[10] Pettigrew, E.D., Shepherd, S.G. Ruohoniemi, J.M. (2010), Climatological patterns of high-latitude convection in the Northern and Southern hemispheres: Dipole tilt dependencies and interhemispheric comparisons, *J. Geophys. Res.*, 115, A07305

[11] Theiler, J., and Prichard, D. (1996), Constrained-realization Monte-Carlo method for hypothesis testing, *Physica D*, 94, 221–235.

[12] Thejll, P., Christiansen, B., and Gleisner, H. (2003), On correlations between the North Atlantic Oscillation, geopotential heights, and geomagnetic activity, *Geophys. Res. Lett.*, 30, 1347

[13] Tinsley, B.A. (2000). Influence of Solar Wind on the Global Electric Circuit, and Inferred Effects on Cloud Microphysics, Temperature, and Dynamics in the Troposphere. *Space Science Reviews*, 94, 231-258

[14] Tinsley, B.A. (2008). The global atmospheric electric circuit and its effect on cloud microphysics. *Reports on Progress in Physics*. 71. 66801-31.

[15] Wilks, D.S. (2016), 'The Stippling Shows Statistically Significant Grid Points": How Research Results are Routinely Overstated and Over interpreted, and What to Do about It. *Bulletin of the American Meteorological Society*. 97

Acknowledgments

We thank the ECMWF (European Center for Medium Weather Forecast) for ERA5 data (https://www.ecmwf.int/en/forecasts/datasets/reanalysis-datasets/era5) and the NASA Goddard Space Center for OMNIWeb database (https://omniweb.gsfc.nasa.gov/). All data used in this study is openly available. The research was funded by the Norwegian Research Council under contracts 223252/F50 (BCSS) and 300724 (EPIC).

JOHN WILEY AND SONS LICENSE
TERMS AND CONDITIONS

Nov 27, 2020

This Agreement between Dr. Spencer Hatch ("You") and John Wiley and Sons ("John Wiley and Sons") consists of your license details and the terms and conditions provided by John Wiley and Sons and Copyright Clearance Center.

License Number	4956990876550
License date	Nov 27, 2020
Licensed Content Publisher	John Wiley and Sons
Licensed Content Publication	Journal of Geophysical Research: Atmospheres
Licensed Content Title	Atmospheric circuit influences on ground-level pressure in the Antarctic and Arctic
Licensed Content Author	A. V. Frank-Kamenetsky, O. A. Troshichev, W. J. R. French, et al
Licensed Content Date	Aug 7, 2008
Licensed Content Volume	113
Licensed Content Issue	D15
Licensed Content Pages	11
Type of use	Another Wiley Imprint/Publication
Requestor type	University/Academic
Is the reuse sponsored by or associated with a pharmaceutical or medical products company?	no

Format	Print and electronic
Portion	Figure/table
Number of figures/tables	2
Will you be translating?	No
Circulation	100
Title of new article	The Mansurov Effect: Real or a statistical artefact?
Lead author	Jone Øvretvedt Edvartsen
Title of targeted journal	Journal of Geophysical Research: Atmospheres
Publisher	John Wiley and Sons
Expected publication date	Feb 2021
Portions	Figure 1, Figure 2
Requestor Location	Dr. Spencer Hatch Birkeland Centre for Space Science Department of Physics and Technology Allégaten 55 Bergen, Hordaland N-5007 Norway Attn: Dr. Spencer Hatch
Publisher Tax ID	EU826007151
Customer VAT ID	NO874789542
Total	0.00 USD
Terms and Conditions	

/

TERMS AND CONDITIONS

This copyrighted material is owned by or exclusively licensed to John Wiley & Sons, Inc. or one of its group companies (each a"Wiley Company") or handled on behalf of a society with which a Wiley Company has exclusive publishing rights in relation to a particular work (collectively "WILEY"). By clicking "accept" in connection with completing this licensing transaction, you agree that the following terms and conditions apply to this transaction (along with the billing and payment terms and conditions established by the Copyright Clearance Center Inc., ("CCC's Billing and Payment terms and conditions"), at the time that you opened your RightsLink account (these are available at any time at http://myaccount.copyright.com).

Terms and Conditions

- The materials you have requested permission to reproduce or reuse (the "Wiley Materials") are protected by copyright.

- You are hereby granted a personal, non-exclusive, non-sub licensable (on a stand-alone basis), non-transferable, worldwide, limited license to reproduce the Wiley Materials for the purpose specified in the licensing process. This license, **and any CONTENT (PDF or image file) purchased as part of your order,** is for a one-time use only and limited to any maximum distribution number specified in the license. The first instance of republication or reuse granted by this license must be completed within two years of the date of the grant of this license (although copies prepared before the end date may be distributed thereafter). The Wiley Materials shall not be used in any other manner or for any other purpose, beyond what is granted in the license. Permission is granted subject to an appropriate acknowledgement given to the author, title of the material/book/journal and the publisher. You shall also duplicate the copyright notice that appears in the Wiley publication in your use of the Wiley Material. Permission is also granted on the understanding that nowhere in the text is a previously published source acknowledged for all or part of this Wiley Material. Any third party content is expressly excluded from this permission.

- With respect to the Wiley Materials, all rights are reserved. Except as expressly granted by the terms of the license, no part of the Wiley Materials may be copied, modified, adapted (except for minor reformatting required by the new Publication), translated, reproduced, transferred or distributed, in any form or by any means, and no derivative works may be made based on the Wiley Materials without the prior permission of the respective copyright owner.**For STM Signatory Publishers clearing permission under the terms of the STM Permissions Guidelines only, the terms of the license are extended to include subsequent editions and for editions in other languages, provided such editions are for the work as a whole in situ and does not involve the separate exploitation of the permitted figures or extracts,** You may not alter, remove or suppress in any manner any copyright, trademark or other notices displayed by the Wiley Materials. You may not license, rent, sell, loan, lease, pledge, offer as security, transfer or assign the Wiley Materials on a stand-alone basis, or any of the rights granted to you hereunder to any other person.

- The Wiley Materials and all of the intellectual property rights therein shall at all times remain the exclusive property of John Wiley & Sons Inc, the Wiley Companies, or their respective licensors, and your interest therein is only that of having possession of and the right to reproduce the Wiley Materials pursuant to Section 2 herein during the continuance of this Agreement. You agree that you own no right, title or interest in or to the Wiley Materials or any of the intellectual property rights therein. You shall have

/

no rights hereunder other than the license as provided for above in Section 2. No right, license or interest to any trademark, trade name, service mark or other branding ("Marks") of WILEY or its licensors is granted hereunder, and you agree that you shall not assert any such right, license or interest with respect thereto

- NEITHER WILEY NOR ITS LICENSORS MAKES ANY WARRANTY OR REPRESENTATION OF ANY KIND TO YOU OR ANY THIRD PARTY, EXPRESS, IMPLIED OR STATUTORY, WITH RESPECT TO THE MATERIALS OR THE ACCURACY OF ANY INFORMATION CONTAINED IN THE MATERIALS, INCLUDING, WITHOUT LIMITATION, ANY IMPLIED WARRANTY OF MERCHANTABILITY, ACCURACY, SATISFACTORY QUALITY, FITNESS FOR A PARTICULAR PURPOSE, USABILITY, INTEGRATION OR NON-INFRINGEMENT AND ALL SUCH WARRANTIES ARE HEREBY EXCLUDED BY WILEY AND ITS LICENSORS AND WAIVED BY YOU.

- WILEY shall have the right to terminate this Agreement immediately upon breach of this Agreement by you.

- You shall indemnify, defend and hold harmless WILEY, its Licensors and their respective directors, officers, agents and employees, from and against any actual or threatened claims, demands, causes of action or proceedings arising from any breach of this Agreement by you.

- IN NO EVENT SHALL WILEY OR ITS LICENSORS BE LIABLE TO YOU OR ANY OTHER PARTY OR ANY OTHER PERSON OR ENTITY FOR ANY SPECIAL, CONSEQUENTIAL, INCIDENTAL, INDIRECT, EXEMPLARY OR PUNITIVE DAMAGES, HOWEVER CAUSED, ARISING OUT OF OR IN CONNECTION WITH THE DOWNLOADING, PROVISIONING, VIEWING OR USE OF THE MATERIALS REGARDLESS OF THE FORM OF ACTION, WHETHER FOR BREACH OF CONTRACT, BREACH OF WARRANTY, TORT, NEGLIGENCE, INFRINGEMENT OR OTHERWISE (INCLUDING, WITHOUT LIMITATION, DAMAGES BASED ON LOSS OF PROFITS, DATA, FILES, USE, BUSINESS OPPORTUNITY OR CLAIMS OF THIRD PARTIES), AND WHETHER OR NOT THE PARTY HAS BEEN ADVISED OF THE POSSIBILITY OF SUCH DAMAGES. THIS LIMITATION SHALL APPLY NOTWITHSTANDING ANY FAILURE OF ESSENTIAL PURPOSE OF ANY LIMITED REMEDY PROVIDED HEREIN.

- Should any provision of this Agreement be held by a court of competent jurisdiction to be illegal, invalid, or unenforceable, that provision shall be deemed amended to achieve as nearly as possible the same economic effect as the original provision, and the legality, validity and enforceability of the remaining provisions of this Agreement shall not be affected or impaired thereby.

- The failure of either party to enforce any term or condition of this Agreement shall not constitute a waiver of either party's right to enforce each and every term and condition of this Agreement. No breach under this agreement shall be deemed waived or excused by either party unless such waiver or consent is in writing signed by the party granting such waiver or consent. The waiver by or consent of a party to a breach of any provision of this Agreement shall not operate or be construed as a waiver of or consent to any other or subsequent breach by such other party.

- This Agreement may not be assigned (including by operation of law or otherwise) by you without WILEY's prior written consent.

- Any fee required for this permission shall be non-refundable after thirty (30) days from receipt by the CCC.

- These terms and conditions together with CCC's Billing and Payment terms and conditions (which are incorporated herein) form the entire agreement between you and WILEY concerning this licensing transaction and (in the absence of fraud) supersedes all prior agreements and representations of the parties, oral or written. This Agreement may not be amended except in writing signed by both parties. This Agreement shall be binding upon and inure to the benefit of the parties' successors, legal representatives, and authorized assigns.

- In the event of any conflict between your obligations established by these terms and conditions and those established by CCC's Billing and Payment terms and conditions, these terms and conditions shall prevail.

- WILEY expressly reserves all rights not specifically granted in the combination of (i) the license details provided by you and accepted in the course of this licensing transaction, (ii) these terms and conditions and (iii) CCC's Billing and Payment terms and conditions.

- This Agreement will be void if the Type of Use, Format, Circulation, or Requestor Type was misrepresented during the licensing process.

- This Agreement shall be governed by and construed in accordance with the laws of the State of New York, USA, without regards to such state's conflict of law rules. Any legal action, suit or proceeding arising out of or relating to these Terms and Conditions or the breach thereof shall be instituted in a court of competent jurisdiction in New York County in the State of New York in the United States of America and each party hereby consents and submits to the personal jurisdiction of such court, waives any objection to venue in such court and consents to service of process by registered or certified mail, return receipt requested, at the last known address of such party.

WILEY OPEN ACCESS TERMS AND CONDITIONS

Wiley Publishes Open Access Articles in fully Open Access Journals and in Subscription journals offering Online Open. Although most of the fully Open Access journals publish open access articles under the terms of the Creative Commons Attribution (CC BY) License only, the subscription journals and a few of the Open Access Journals offer a choice of Creative Commons Licenses. The license type is clearly identified on the article.

The Creative Commons Attribution License

The Creative Commons Attribution License (CC-BY) allows users to copy, distribute and transmit an article, adapt the article and make commercial use of the article. The CC-BY license permits commercial and non-

Creative Commons Attribution Non-Commercial License

The Creative Commons Attribution Non-Commercial (CC-BY-NC)License permits use, distribution and reproduction in any medium, provided the original work is properly cited and is not used for commercial purposes.(see below)

Creative Commons Attribution-Non-Commercial-NoDerivs License